



First results from the Spatial Heterodyne Imager for Mesospheric Radicals (SHIMMER): Diurnal variation of mesospheric hydroxyl

Christoph R. Englert,¹ Michael H. Stevens,¹ David E. Siskind,¹ John M. Harlander,² Fred L. Roesler,³ Herbert M. Pickett,⁴ Christian von Savigny,⁵ and Andrew J. Kochenash⁶

Received 21 July 2008; revised 22 August 2008; accepted 28 August 2008; published 8 October 2008.

[1] We present the first SHIMMER observations of the diurnal variation of mesospheric hydroxyl (OH). We compare our data with Aura Microwave Limb Sounder (MLS) observations at about 13h local time near 55°N and find very good agreement. This validates the Spatial Heterodyne Spectroscopy technique for space-borne optical remote sensing applications. We extend our analysis to other local times, not observed by MLS, for latitudes near 55°N in the summer of 2007. At 74 km, we find excellent agreement with a photochemical model, but above 76 km, significant model/data differences in the shape of the OH diurnal variation are observed.

Citation: Englert, C. R., M. H. Stevens, D. E. Siskind, J. M. Harlander, F. L. Roesler, H. M. Pickett, C. von Savigny, and A. J. Kochenash (2008), First results from the Spatial Heterodyne Imager for Mesospheric Radicals (SHIMMER): Diurnal variation of mesospheric hydroxyl, *Geophys. Res. Lett.*, 35, L19813, doi:10.1029/2008GL035420.

1. Introduction

[2] In the mesosphere, hydroxyl (OH) is predominantly produced by the photodissociation of water vapor (H₂O) and its use as a proxy for mesospheric H₂O has been demonstrated [Summers *et al.*, 1997, 2001]. Measurements of mesospheric hydroxyl (OH) have been performed from aircraft, balloons, and satellites. The aircraft measurements, using far infrared emission, were limited to a vertical resolution of about 25 km in the mesosphere [Englert *et al.*, 2000]. Balloon measurements have provided column densities above about 40 km [Pickett *et al.*, 2006a]. Recently, only four instruments in Earth orbit have been capable of providing high vertical resolution OH altitude profiles in the mesosphere: The Imaging Spectrometric Observatory (ISO) [Morgan *et al.*, 1993], the Middle Atmospheric High Resolution Spectrograph Investigation (MAHRSI) [Conway *et al.*, 1999], the Optical Spectrograph and Infrared Imager System (OSIRIS) [Gattinger *et al.*, 2006], and the Micro-

wave Limb Sounder (MLS) on Aura [Pickett *et al.*, 2006a, 2006b, 2008].

[3] ISO OH data was reported for one day, one latitude, and one local time. The MAHRSI data are limited to two Space Shuttle flights in 1994 and 1997 which provided very little local time (LT) coverage for any given latitude and both OSIRIS and MLS observations are made from sun synchronous platforms that essentially sample only two local times. In contrast, the Spatial Heterodyne Imager for Mesospheric Radicals (SHIMMER) measures mesospheric OH over the diurnal cycle and the first results are discussed here. Like the diurnal measurements of HO₂, O₃ and H₂O, SHIMMER data are expected to be an invaluable tool to assess our understanding of the processes describing mesospheric HO_x (HO₂, OH, H) [Sandor and Clancy, 1998].

[4] SHIMMER was launched on board the Space Test Program Satellite-1 (STPSat-1) on March 9, 2007. It measures the OH solar resonance fluorescence by observing the A²Σ⁺–X²Π(0,0) band near 309 nm. SHIMMER uses the innovative Spatial Heterodyne Spectroscopy technique which offers considerable advantages in reducing size and weight compared to conventional grating spectrographs [Harlander *et al.*, 2003]. SHIMMER has no moving optical components and images the Earth's limb, rather than scanning it. The STPSat-1 orbital inclination and orbit altitude result in observations up to 58° latitude with a local time precession of ~30 minutes per day, allowing SHIMMER to measure over the diurnal cycle [Stevens *et al.*, 2008].

[5] In this study, we first compare the SHIMMER OH measurements with MLS data at the local time of the MLS measurements (~13h). Subsequently, we investigate the local time variation of OH as measured by SHIMMER in the upper mesosphere and compare to results from a one-dimensional photochemical model.

2. SHIMMER Observations

[6] The STPSat-1 satellite is in a 35.4° orbital inclination and the SHIMMER field of view is oriented perpendicular to the satellite velocity direction towards the summer pole so that it observes to about 58° latitude. It typically images the limb between ~33–97 km altitude, with 2 km altitude sampling, a 12 second integration time, and a sampling period of 20 seconds. SHIMMER measurements provide very dense coverage within the 53°N–58°N latitude band in the northern summer, with over 500 limb images per day [Stevens *et al.*, 2008]. We therefore focus on this latitude region for our comparison with MLS data and model results.

[7] The raw SHIMMER interferograms are downlinked and processed on the ground. The dark field correction is

¹Space Science Division, Naval Research Laboratory, Washington, D. C., USA.

²Department of Physics, Astronomy and Engineering Science, Saint Cloud State University, St. Cloud, Minnesota, USA.

³Department of Physics, University of Wisconsin-Madison, Madison, Wisconsin, USA.

⁴Jet Propulsion Laboratory, California Institute of Technology, Pasadena, California, USA.

⁵Institute of Environmental Physics and Remote Sensing, University of Bremen, Bremen, Germany.

⁶Computational Physics Incorporated, Springfield, Virginia, USA.

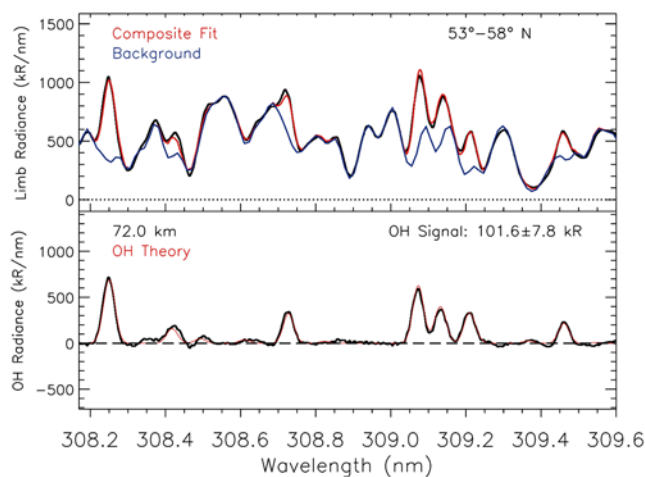


Figure 1. (top) Averaged SHIMMER spectrum at 72 km tangent altitude (black). Fitted spectrum including the Rayleigh scattered solar background and the OH emission lines (red). Estimated Rayleigh scattered background (blue). (bottom) Difference between the measured spectrum and the Rayleigh scattered background (black). Fitted OH emission lines (red).

performed using on-orbit measurements, the flat-field correction is performed applying the unbalanced arm flat-fielding approach [Englert and Harlander, 2006] based on laboratory measurements, and the phase correction assumes a low resolution phase shift [Englert et al., 2004]. Furthermore, corrections for cosmic ray effects on the detector, thermal defocus, and grating imperfections are applied. The radiometric calibration is based on laboratory measurements using a National Institute of Standards and Technology (NIST) traceable UV light source. A representative, averaged spectrum for a tangent point height of 72 km is shown as the black line in Figure 1 (top).

[8] The separation of the OH resonance fluorescence signal from the Rayleigh scattered background is performed using a method that is similar to the one used for the MAHRSI data [Conway et al., 1999]. This includes fitting the spectral shapes of the OH emission, the Rayleigh scattered solar flux, a baseline offset, and the instrumental line shape function. The solar background shape was obtained from on-orbit SHIMMER measurements of direct sunlight. A limb observation at 72 km, the estimated background and the best fit of the total signal are shown in Figure 1 (top). The measured signal after the subtraction of the background and the fitted OH emission spectrum, convolved with the instrumental line shape function are shown in the bottom panel. We determine the brightness of the OH emission for each altitude using this proven approach.

[9] The altitude registration of the limb images is achieved using the satellite position and attitude data as measured by the on-board Global Positioning System and star tracker. SHIMMER does not have the capability to verify the pointing accuracy with on-orbit observations of known targets like stars. Therefore, in order to correct for any systematic errors in the alignment of the star tracker with respect to SHIMMER, including the on-orbit thermo-elastic distortion of the satellite, we employ the Tangent Height Retrieval by UV-B Exploitation (TRUE) method,

which has previously demonstrated an accuracy of better than 1 km [von Savigny et al., 2005]. Using a subset of SHIMMER data used for this work, we find an altitude offset of 2.81 ± 0.35 km, which we apply to the data.

[10] To retrieve the OH altitude concentration profile from the OH brightness profile we use a Twomey regularized least squares method as described by Conway et al. [1999]. Our version is nearly identical to the algorithm that was used for the MAHRSI data analysis [Summers et al., 1997, 2001; Conway et al., 1999, 2000], including the same OH(0,0) emission rate factors (g factors) [Stevens and Conway, 1999]. The main difference is that the analysis is adjusted for the slightly smaller SHIMMER passband.

3. Comparison of SHIMMER and MLS OH Observations

[11] To compare SHIMMER OH results with another coincident measurement, we use observations from the MLS instrument on NASA's Aura satellite. We choose data from July 16, 2007 during which the two instruments were observing the limb at the same local time. We take a zonal average of SHIMMER data (version 1.0) at 12.6 ± 2.6 hours LT and a zonal average of MLS data (version 2.21) at 12.8 hours LT between 53–58°N. Figure 2 illustrates the comparison of the observations between 60–90 km altitude with shaded envelopes representing the combined 1σ statistical and systematic uncertainties. The SHIMMER uncertainty is the root sum square (rss) of an altitude dependent statistical error derived from the baseline variation in the spectrum, systematic errors that are predominantly due to the correction of grating imperfections and a 7% rss uncertainty in the OH g factors [Conway et al., 1999]. The MLS uncertainty includes the statistical error and a 10% systematic error. The agreement is excellent, especially considering that the two observations use completely different remote sensing techniques.

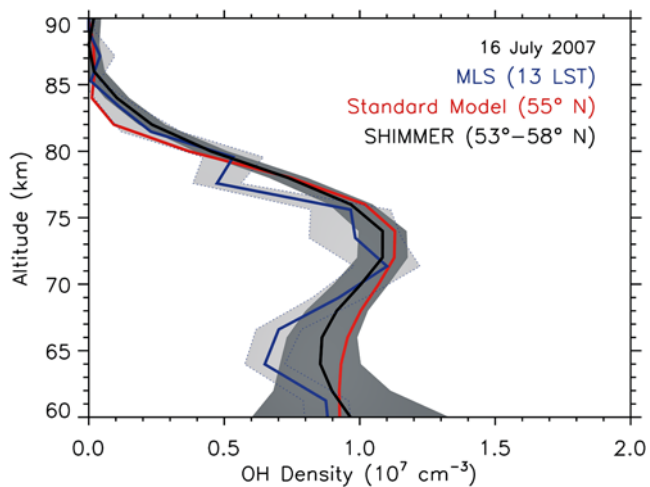


Figure 2. Comparison of OH vertical density profiles measured by SHIMMER (black) and MLS (blue) and calculated by the NRL-CHEM1D photochemical model (red). The model result is multiplied with the SHIMMER weighting functions to match the altitude resolution. The model result is initialized with MLS H₂O for the same day, latitudes and local time.

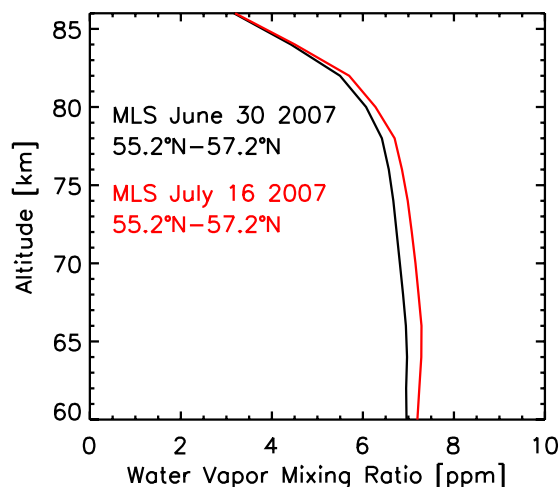


Figure 3. Water vapor profiles measured by MLS for July 16, 2007 and June 30, 2007. The profiles show only small differences (less than $\pm 10\%$) between 60–85 km.

[12] Also shown in Figure 2 is the result of an NRL-CHEM1D photochemical model calculation [Summers *et al.*, 1997, 2001] using standard JPL06 reaction rates [Sander *et al.*, 2006], MLS H_2O (Version 2.2) [Lambert *et al.*, 2007], temperature, and pressure profiles for the same latitude range. The zonally averaged MLS water vapor profile for July 16 used in the model calculation is shown in red in Figure 3. SHIMMER OH data between 60–90 km are in good agreement with the model. This is in contrast to MAHRSI observations of solar resonance fluorescence, which indicated a 25–30% model overprediction in the mesosphere [Conway *et al.*, 1999, 2000].

[13] It is important to note that while the averaging kernels for SHIMMER OH and MLS OH are 3–7 km wide between 65–90 km, the averaging kernels for the MLS H_2O are between 11–16 km wide [Lambert *et al.*, 2007].

[14] Figure 2 also serves as a verification that the SHIMMER OH measurement does not suffer from a significant scattered light problem. In addition to the good agreement between SHIMMER and MLS results, the retrieved OH density approaches zero above 85 km, which confirms that OH signal from below does not contaminate the higher altitudes.

4. Mesospheric OH Over the Diurnal Cycle

[15] The local time precession of the SHIMMER measurements allows us to investigate the diurnal variation of OH, which we accomplish by comparing zonally averaged SHIMMER data with results of the NRL-CHEM1D model. We use zonally averaged SHIMMER OH profiles between 55–58°N and between 27 June and 2 August, 2007, during which the average local time decreased monotonically from 20.6 to 5.1 hours. The results are shown in Figure 4 for six altitudes between 74 km and 84 km. The SHIMMER points are 3 day averages, resulting in one data point every ~ 1.5 h LT. OH observations after 20.6 h and before 5.1 h LT are not shown due to the lack of sunlight required for the fluorescence observations.

[16] For the model results, we use zonally averaged MLS H_2O profiles for the same latitude region and time periods

measured at about 13 h LT. The individual water profiles show only small changes during this period as indicated by the two profiles for June 30 and July 16 in Figure 3.

[17] At 74 km the agreement between the SHIMMER OH data and NRL-CHEM1D is excellent. Here, the shape of the diurnal variation is dominated by the variation of the OH production by photodissociation of water, which is a function of the solar zenith angle. Therefore, the OH concentration peaks around local noon, for the smallest solar zenith angle.

[18] Above 76 km, on the other hand, the measured shape of the diurnal variation is significantly different from the model results. At these altitudes, the modeled OH peaks later in the afternoon, resulting from the interaction of the

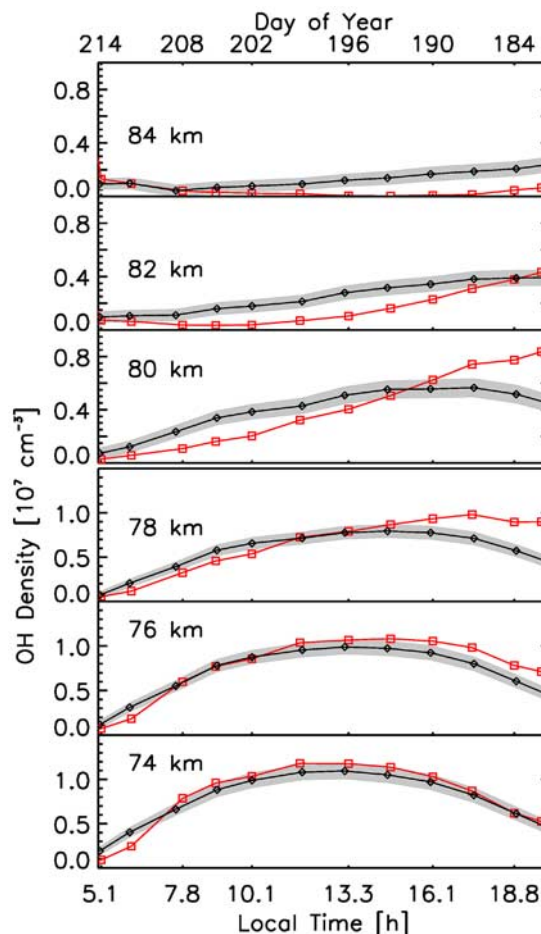


Figure 4. Diurnal behavior of OH as measured by SHIMMER (black diamonds) compared with CHEM1D calculations (red squares). The error envelope of the SHIMMER measurements reflects an estimate of the combined 1σ systematic and statistical uncertainties. SHIMMER local times vary from 20.6 h on 27 June (Day 178) to 5.1 h on 2 August (Day 214). The CHEM1D curves represent a composite of 12 separate calculations for the dates indicated by the top axis. Each calculation uses the zonal average MLS H_2O profile at ~ 13 h LT for the same latitude region (55–58°N). Each red square represents the model result for the local time given by the bottom axis. The model results are smoothed with the SHIMMER altitude resolution.

HO_x species with ozone [e.g., Prather, 1981; Summers *et al.*, 2001]. SHIMMER, however, shows a systematically different shape of the diurnal variation with absolute density differences of two or more, which is well beyond the uncertainties.

5. Discussion and Conclusions

[19] We have compared mesospheric OH density profiles of SHIMMER and MLS for the same day, the same latitudes and at the same local time. The results are in excellent agreement, proving that the innovative SHS optical technique is valuable for long duration space-borne UV remote sensing.

[20] We have also compared SHIMMER and MLS OH observations near 13LT with results from a one-dimensional photochemical model using standard JPL06 chemistry, where the model is initialized with MLS H₂O. We find that both SHIMMER and MLS data are in good agreement with the model results.

[21] Finally, we have presented the first satellite observations of mesospheric OH over nearly the entire diurnal cycle and here we find discrepancies with the model above 76 km. In an effort to reconcile these differences we considered the reaction rate uncertainty of the dominant reaction which partitions OH and H (H+O₃→OH+O₂) [Mlynczak *et al.*, 1998] and which is of particular importance in the altitude region where we see the differences. We scaled this rate by ±50% which is about twice the uncertainty given by Sander *et al.* [2006] and found that the OH around 80 km responded significantly, but it did not improve the model/data comparison. Furthermore, diurnally varying temperatures due to tides increasingly become more important at the higher altitudes. Likewise, because H₂O has a strong vertical gradient at 80 km, it too should vary with tidal upwelling and downwelling; however, the magnitude of the OH model-data discrepancy is too large to be remedied by a simple scaling of the H₂O model input. Also, the HO_x chemical lifetime is increasing rapidly above ~80 km [Brasseur and Solomon, 1986] suggesting that transport effects may play a role. Our model calculations shown here did not explicitly account for diffusive transport; however, a test simulation with vertical eddy diffusion (K_{zz}) confirmed that it can be of importance at these altitudes. Finally, since these SHIMMER measurements are made at the fringe region of noctilucent clouds, the redistribution of H₂O through ice particle growth and sublimation might be relevant [Murray and Plane, 2005].

[22] A detailed parametric study of all these factors is beyond the scope of the present paper. We suggest that the high quality of the SHIMMER data with its substantial diurnal and seasonal coverage (as of this writing, SHIMMER observations have covered more than one year), combined with other observations such as that of O₃ and temperature from SABER on TIMED [Huang *et al.*, 2008] would be invaluable in providing new insights about the roles of chemistry and dynamics in the upper mesosphere over the diurnal cycle.

[23] **Acknowledgments.** Funding for this research was provided by the Office of Naval Research. SHIMMER is a joint program between the Naval Research Laboratory and the DoD Space Test Program. The authors would like to thank Joel G. Cardon, Ronen Feldman, John F. Moser,

W. Layne Marlin, Charles M. Brown, Robert R. Conway, Andrew N. Straatveit, Michael A. Carr, and Andrew W. Stephan for their contributions to the SHIMMER project. Research at the Jet Propulsion Laboratory, California Institute of Technology, was performed under contract with NASA.

References

- Brasseur, G., and S. Solomon (1986), *Aeronomy of the Middle Atmosphere*, 2nd ed., D. Reidel, Dordrecht, Netherlands.
- Conway, R. R., M. H. Stevens, C. M. Brown, Joel G. Cardon, S. E. Zasadil, and G. H. Mount (1999), Middle atmosphere high resolution spectrograph investigation, *J. Geophys. Res.*, *104*, 16,327–16,348.
- Conway, R. R., M. E. Summers, M. H. Stevens, J. G. Cardon, P. Preusse, and D. Offermann (2000), Satellite observations of upper stratospheric and mesospheric OH: The HO_x dilemma, *Geophys. Res. Lett.*, *27*, 2613–2616.
- Englert, C. R., and J. M. Harlander (2006), Flatfielding in spatial heterodyne spectroscopy, *Appl. Opt.*, *45*, 4583–4590.
- Englert, C. R., B. Schimpf, M. Birk, F. Schreier, M. Krocka, R. G. Nitsche, R. U. Titz, and M. E. Summers (2000), The 2.5 THz heterodyne spectrometer THOMAS: Measurement of OH in the middle atmosphere and comparison with photochemical model results, *J. Geophys. Res.*, *105*, 22,211–22,223.
- Englert, C. R., J. M. Harlander, J. G. Cardon, and F. L. Roesler (2004), Correction of phase distortion in spatial heterodyne spectroscopy, *Appl. Opt.*, *43*, 6680–6687.
- Gattinger, R. L., D. A. Degenstein, and E. J. Llewellyn (2006), Optical Spectrograph and Infra-Red Imaging System (OSIRIS) observations of mesospheric OH A²Σ⁺-X²Π 0-0 and 1-1 band resonance emissions, *J. Geophys. Res.*, *111*, D13303, doi:10.1029/2005JD006369.
- Harlander, J. M., F. L. Roesler, C. R. Englert, J. G. Cardon, R. R. Conway, C. M. Brown, and J. Wimperis (2003), Robust monolithic ultraviolet interferometer for the SHIMMER instrument on STPSat-1, *Appl. Opt.*, *42*, 2829–2834.
- Huang, F. T., H. G. Mayr, J. M. Russell III, M. G. Mlynczak, and C. A. Reber (2008), Ozone diurnal variations and mean profiles in the mesosphere, lower thermosphere, and stratosphere, based on measurements from SABER on TIMED, *J. Geophys. Res.*, *113*, A04307, doi:10.1029/2007JA012739.
- Lambert, A., *et al.* (2007), Validation of the Aura Microwave Limb Sounder middle atmosphere water vapor and nitrous oxide measurements, *J. Geophys. Res.*, *112*, D24S36, doi:10.1029/2007JD008724.
- Mlynczak, M. G., D. K. Zhou, and S. M. Adler-Golden (1998), Kinetic and spectroscopic requirements for the inference of chemical heating rates and atomic hydrogen densities from OH Meinel band measurements, *Geophys. Res. Lett.*, *25*, 647–650.
- Morgan, M. F., D. G. Torr, and M. R. Torr (1993), Preliminary measurements of mesospheric OH X²Π by ISO on ATLAS 1, *Geophys. Res. Lett.*, *20*, 511–514.
- Murray, B. J., and J. M. C. Plane (2005), Modelling the impact of noctilucent cloud formation on atomic oxygen and other minor constituents of the summer mesosphere, *Atmos. Chem. Phys.*, *5*, 1027–1038.
- Pickett, H. M., B. J. Drouin, T. Canty, L. J. Kovalenko, R. J. Salawitch, N. J. Livesey, W. G. Read, J. W. Waters, K. W. Jucks, and W. A. Traub (2006a), Validation of Aura MLS HO_x measurements with remote-sensing balloon instruments, *Geophys. Res. Lett.*, *33*, L01808, doi:10.1029/2005GL024048.
- Pickett, H. M., W. G. Read, K. K. Lee, and Y. L. Yung (2006b), Observation of night OH in the mesosphere, *Geophys. Res. Lett.*, *33*, L19808, doi:10.1029/2006GL026910.
- Pickett, H. M., *et al.* (2008), Validation of Aura Microwave Limb Sounder OH and HO₂ measurements, *J. Geophys. Res.*, *113*, D16S30, doi:10.1029/2007JD008775.
- Prather, M. J. (1981), Ozone in the upper stratosphere and mesosphere, *J. Geophys. Res.*, *86*, 5325–5338.
- Sander, S. P., *et al.* (2006), Chemical kinetics and photochemical data for use in atmospheric studies, *JPL Publ.*, 06-2.
- Sandor, B. J., and R. T. Clancy (1998), Mesospheric HO_x chemistry from diurnal microwave observations of HO₂, O₃, and H₂O, *J. Geophys. Res.*, *103*, 13,337–13,351.
- Stevens, M. H., and R. R. Conway (1999), Calculated OH A²Σ⁺-X²Π (0,0) band rotational emission rate factors for solar resonance fluorescence, *J. Geophys. Res.*, *104*, 16,369–16,378.
- Stevens, M. H., C. R. Englert, M. Hervig, S. V. Petelina, W. Singer, and K. Nielsen (2008), The diurnal variation of polar mesospheric cloud frequency near 55°N observed by SHIMMER, *J. Atmos. Solar-Terr. Phys.*, in press.
- Summers, M. E., R. R. Conway, D. E. Siskind, M. H. Stevens, D. Offermann, M. Riese, P. Preusse, D. F. Strobel, and J. M. Russell III (1997), Implications of satellite OH observations for middle atmospheric H₂O and ozone, *Science*, *277*, 1967–1969.

- Summers, M. E., R. R. Conway, C. R. Englert, D. E. Siskind, M. H. Stevens, J. M. Russell III, L. L. Gordley, and M. J. McHugh (2001), Discovery of enhanced water vapor in the Arctic summer mesosphere: Implications for polar mesospheric clouds, *Geophys. Res. Lett.*, *28*, 3601–3604.
- von Savigny, C., et al. (2005), Spatial and temporal characterization of SCIAMACHY limb pointing errors during the first three years of the mission, *Atmos. Chem. Phys.*, *5*, 2593–2602.
-
- C. R. Englert, D. E. Siskind, and M. H. Stevens, Space Science Division, Naval Research Laboratory, 4555 Overlook Avenue SW, Code 7641, Washington, DC 20375, USA. (christoph.englert@nrl.navy.mil)
- J. M. Harlander, Department of Physics, Astronomy and Engineering Science, Saint Cloud State University, St. Cloud, MN 56301, USA.
- A. J. Kochenash, Computational Physics Incorporated, 8001 Braddock Road, Suite 210, Springfield, VA 22151, USA.
- H. M. Pickett, Jet Propulsion Laboratory, California Institute of Technology, 4800 Oak Grove Drive, Mail Stop 183-701, Pasadena, CA 91109, USA.
- F. L. Roesler, Department of Physics, University of Wisconsin-Madison, Madison, WI 53706, USA.
- C. von Savigny, Institute of Environmental Physics and Remote Sensing, University of Bremen, D-28359 Bremen, Germany.